

Causality violation and the speed of sound of hot and dense quark matter in the Nambu–Jona-Lasinio model

Arthur E.B. Pasqualotto,^{1,*} Ricardo L. S. Farias,^{1,†} William R. Tavares,^{2,3,‡} Sidney S. Avancini,^{2,§} and Gastão Krein^{4,¶}

¹*Departamento de Física, Universidade Federal de Santa Maria, 97105-900 Santa Maria, RS, Brazil*

²*Departamento de Física, Universidade Federal de Santa Catarina, 88040-900 Florianópolis, SC, Brazil*

³*Departamento de Física Teórica, Universidade do Estado do Rio de Janeiro, 20550-013 Rio de Janeiro, RJ, Brazil*

⁴*Instituto de Física Teórica, Universidade Estadual Paulista,*

Rua Dr. Bento Teobaldo Ferraz, 271 - Bloco II, 01140-070 São Paulo, São Paulo, Brazil

The Nambu–Jona-Lasinio model is widely used to study strong-interaction phenomena in vacuum and quark matter. Since the model is nonrenormalizable, one needs to work within a specific regularization scheme to obtain finite results. Here we show that a commonly used cutoff regularization scheme leads to unphysical results, such as superluminal speed of sound and wrong high-temperature behavior of the specific heat and other thermodynamical quantities. Such a troublesome feature of the cutoff regularization invalidates the model for temperature and baryon density values relevant to the phenomenology of heavy-ion collisions and compact stars. We show that the source of the problems stems from cutting off momentum modes in finite integrals depending on thermal distribution functions in the grand canonical potential. The problems go away when taking into account the full momentum range of those integrals. Explicit examples are worked out in the SU(2)-flavor version of the model.

I. INTRODUCTION

Signals of a phase change, from a cold and low-density hadronic phase to a hot and low-density quark-gluon phase, has been identified in several observables collected from heavy-ion collision experiments at the Relativistic Heavy Ion Collider (RHIC) and the Large Hadron Collider; Refs. [1–3] provide reviews with extensive lists of references. A basic quantity characterizing new phases of matter produced in heavy-ion collisions is the equation of state (EOS) [4]. From the EOS, one can compute the speed of sound c_s , which can be used to identify phase changes in the matter produced in those collisions [5]. The speed of sound is also relevant in the study of the cold and dense matter found in compact stars; c_s controls the stiffness of the EOS [6–15], a property that constrains the mass-radius relation of such stars [16–34].

Quantum chromodynamics (QCD) is the fundamental theory governing strongly interacting matter. A first-principles QCD computation of the EOS at finite temperatures has been performed with lattice QCD simulations using Monte Carlo methods. But when dealing with matter at baryon densities relevant to compact stars, neutron stars in particular, sign problems obstruct the use of those methods and alternative theoretical methods are required. At low baryon densities n_B , densities much smaller than the nuclear saturation density $n_0 = 0.16 \text{ fm}^{-3}$, it is possible to construct an EOS with chiral perturbation theory (ChPT) [24, 35, 36] or through many-body nuclear models and constraints from experimental data [12]. In the very-high-density regime, e.g., $n_B \gtrsim 40n_0$, the QCD asymptotic freedom property enables the use of weak-coupling

perturbation theory [12, 37–40]. Computations using this approach [38, 40] found a value for the speed of sound below the conformal limit $c_s^2 = 1/3$, as expected for low-density matter. In the intermediate-density regime, relevant for the phenomenology of neutron stars, interpolation and extrapolation strategies have been used; for a recent review, see Ref. [41]. For such densities, there is an ongoing debate [17, 23, 42–44] regarding the upper bound of c_s^2 .

The speed of sound has also been computed at finite temperature and chemical potential in several contexts using different phenomenological approaches. This is the case of heavy-ion collisions, where the entropy per baryon, s/n_B , is approximately constant in the whole expansion stage of the collision [45]. Estimations of entropy per baryon have been obtained within the range $s/n_B = 17.5$ and 331.6 for collisions with center-of-mass energy in the range between $\sqrt{s_{NN}} = 7.7$ and 200 GeV [46], with data provided by the STAR Collaboration in Refs. [47, 48]. Another example is the envisaged experiments at the Nuclotron-based Ion Collider fAcility, at which it is expected to obtain entropy to baryon density ratios in the range $s/n_B = 4 - 11$ with the collision energies in the range $\sqrt{s_{NN}} = 4 - 11 \text{ GeV}$ [49]. In the context of Taylor expansion coefficients in lattice QCD, it is possible to construct an EOS with values of s/n_B in the range $s/n_B \sim 30 - 300$ for the conditions achieved in experiments at the RHIC, SPS, and AGS [45, 50, 51]. Lower values of s/n_B can be obtained looking at the different stages of formation of a proto-neutron star described in terms of isentropic lines [52–56]. In the first stage, where $s/n_B \sim 1$, there is an abundance of trapped neutrinos, followed by the process of deleptonization, where the star reaches its maximum inner temperature with $s/n_B \sim 2$. In the final stage, with the tendency of the diffusion of neutrinos and cooling, the star can reach $s/n_B \sim 0$.

Alternatively to the high temperature and/or chemical potential systems, there are other environments that are explored in the context of heavy-ion collisions. Because of the nontrivial structure of QCD vacuum at high temperatures, classical solutions called sphalerons take place [57, 58] and can in-

* arthur.pasqualotto@acad.ufsm.br

† ricardo.farias@ufsm.br

‡ william.tavares@posgrad.ufsc.br

§ sidney.avancini@ufsc.br

¶ gastao.krein@unesp.br

duce, through the Adler-Bell-Jackiw anomaly, an imbalance between right-handed and left-handed quarks. Such configurations can be present in C and CP [59, 60] violating processes. Such a situation can happen in the quark-gluon plasma when a strong magnetic field perpendicular to the reaction plane is produced in a peripheral heavy-ion collision [61], generating a vector current in the same direction. This effect is known as the chiral magnetic effect [59], and has been extensively explored theoretically and experimentally [62–67]. Some of these aspects encouraged the investigation of the effects in the effective quark masses and chiral density in the context of parallel electromagnetic fields [68, 69]. Neutron stars, in principle, could be affected by the chiral imbalance since they are subject to high densities and/or strong magnetic fields [70]. Furthermore, lattice QCD simulations of a chiral-imbalanced medium, with the imbalance set by a chiral chemical potential μ_5 , do not suffer from the sign problem [71], a welcome feature for comparisons of effective models [72].

These different high-density scenarios impose technical difficulties in their modeling with a nonrenormalizable model, as for example with the SU(2) Nambu–Jona-Lasinio (NJL) model [73–75] and its extensions to more flavors [76, 77]. The NJL model has been widely used to study several aspects related to the QCD chiral transition, in vacuum, in matter at finite temperature and density [75–77] and external magnetic field [78]. Since the model is nonrenormalizable, the regularization scheme becomes part of the model, in that the regulator cannot be removed. However, careless use of a regularization scheme can lead to gross violations of basic physical principles. This happens with one of the most used regulation schemes, namely, cutoff regularization, or traditional regularization scheme (TRS) [72], in which divergent integrals are regulated with a momentum cutoff Λ . In the present paper, we show that this regularization scheme, as used in many publications, e.g. [79–88], can lead to causality violation through a superluminal speed of sound of quark matter and can also lead to a conformality violation and wrong behavior of the specific heat and other thermodynamic quantities at high temperatures. We show that the source of such troublesome features is related to the use of a cutoff in finite integrals in the grand canonical potential. A known example is the Stefan-Boltzmann limit of thermodynamical quantities. One obtains the Stefan-Boltzmann limit only when the finite thermal contributions depending on the Fermi-Dirac distributions are integrated over the full momentum range [89–91]; the Stefan-Boltzmann limit is not obtained when those contributions are integrated with the same ultraviolet cutoff Λ used to regulate divergent integrals [92].

Similar problems are normally ignored when considering finite-density and chiral-imbalanced systems. For chiral-imbalanced systems modeled within the NJL model with a chiral chemical potential μ_5 , there exist just a few works concerning the role of regularization prescriptions. The importance of an adequate regularization resides in the fact that the vacuum contribution of the thermodynamical potential in the NJL model turns out to be entangled with a contribution depending on the chiral chemical potential μ_5 in a divergent contribution. One can get finite results adopting the TRS

scheme [85]. However, such a scheme [85, 93, 94] leads to results in disagreement with the lattice QCD simulations of Refs. [95, 96]; this is also true when using the TRS in PNJL models [97–99]. It is worth mentioning that the linear sigma model coupled to quarks [97, 100], which is a renormalizable model, also leads to results disagreeing with those lattice results. One can get agreement with the lattice results when one uses the regularization named medium separation scheme [72], in that one separates the vacuum contributions from the medium. Besides all of these issues, the chiral chemical potential can also induce divergences in the chiral charge density, due to the nonconservation of the chiral current in the physical limit, which imposes a normalization procedure [70, 101]. There are some other applications studying the chiral symmetry restoration and the QCD phase diagram with different approaches and models in Refs. [87, 102–104].

In this work, guided by all this phenomenology, we study within an SU(2) NJL model the effects of regulating or not with of an ultraviolet cutoff finite integrals contributing to the thermodynamic potential of quark matter under two scenarios: finite quark chemical potential and the chiral chemical potential. The isentropic lines are obtained in both $T - \mu_q$ and $T - \mu_5$ planes and the speed of sound is calculated. To this end, we present in Sec. II the formalism of the SU(2) NJL model at finite temperature and chemical potential. We present the explicit expressions for the thermodynamical quantities depending on T and μ_q in Sec. II. A, and those depending on T and μ_5 in Sec. II. B. We present numerical results in Sec. III. In Sec. IV we present our conclusions.

II. NJL MODEL AT FINITE TEMPERATURE AND DENSITY

We use a NJL model defined by the following Lagrangian density [73–77]:

$$\mathcal{L}_{\text{NJL}} = \bar{\psi} (i\cancel{\partial} - \hat{m}) \psi + G [(\bar{\psi}\psi)^2 + (\bar{\psi}i\gamma_5\tau\psi)^2], \quad (1)$$

where $\psi = (u \ d)^T$ represents the u (up) and d (down) quark isospin doublet, $\hat{m} = \text{diag}(m_u \ m_d)$ is the quark mass matrix, G the coupling strength, and $\tau = (\tau^1, \tau^2, \tau^3)$ are the isospin Pauli matrices.

Like with most quantum field theoretical models, ultraviolet divergences occur in the process of calculating physical quantities within the NJL model. In order to give physical sense to the results derived from the model, one needs a regularization procedure. Since the NJL model is nonrenormalizable, the regularization procedure becomes an integral part of the model. In this work, we employ a three-dimensional momentum cutoff scheme, by far the most frequently used scheme in the NJL model. We refer to it as the traditional regularization scheme (TRS), a previously defined nomenclature [72].

In the following, we present the derivation of the expressions for the thermodynamical quantities within the TRS. We consider first the expressions for quark matter at finite-temperature T and quark baryon chemical potential μ_q . Next, we derive the expressions for quark matter at finite T and

a chiral imbalance of right- and left-handed quarks by fixing the imbalance with a quark chiral chemical potential μ_5 . The chemical potentials enter in the grand canonical potential Ω , from which one derives the thermodynamical quantities. In the imaginary time formalism of finite temperature field theory, one incorporates μ_q and μ_5 by adding to the Euclidean action corresponding to the Lagrangian density \mathcal{L}_{NJL} the following terms:

$$S_{\mu_q} = \int_0^\beta d\tau \int d^3x \bar{\psi} \mu_q \gamma_0 \psi, \quad (2)$$

$$S_{\mu_5} = \int_0^\beta d\tau \int d^3x \bar{\psi} \mu_5 \gamma_0 \gamma_5 \psi, \quad (3)$$

with the quark fields obeying antiperiodic boundary conditions in $\beta = 1/T$, namely, $\psi(\mathbf{x}, 0) = -\psi(\mathbf{x}, \beta)$. We compute Ω in the mean-field approximation and work in the isospin symmetry limit $m_u = m_d = m_0$.

The thermodynamical quantities of interest in this paper are the speed of sound c_s , specific heat c_V , interaction strength (or trace anomaly) Δ , and conformal measure C . They are defined in terms of partial derivatives of quantities defining the EOS, the pressure $P = -\Omega$, the energy density ϵ , the entropy density s and quark number density ρ :

$$P_N = P(T, \mu) - P(0, 0), \quad (4)$$

$$\epsilon = -P_N + Ts + \mu\rho, \quad (5)$$

$$s = -\left(\frac{\partial\Omega}{\partial T}\right)_\mu, \quad \rho = -\left(\frac{\partial\Omega}{\partial\mu}\right)_T, \quad (6)$$

where $M = M(T, \mu)$ is the constituent quark mass, the solution of the gap equation. Here, μ stands for either μ_q or μ_5 and thereby ρ stands for ρ_q or ρ_5 , respectively. From these, one can then readily compute c_s , c_V , Δ , and C as follows:

$$c_s^2 = -\left(\frac{\partial P_N}{\partial\epsilon}\right)_{s/\rho} = \frac{\rho^2 \Upsilon_{T,T} - 2(s\rho) \Upsilon_{T,\mu} - s^2 \Upsilon_{\mu,\mu}}{(\epsilon + P_N)(\Upsilon_{T,T} \Upsilon_{\mu,\mu} - \Upsilon_{\mu,T}^2)}, \quad (7)$$

$$c_V = \left(\frac{\partial\epsilon}{\partial T}\right)_\rho = T \left(\frac{\partial s}{\partial T}\right) = T \left(\Upsilon_{T,T} - \frac{\Upsilon_{\mu,T}^2}{\Upsilon_{\mu,\mu}}\right), \quad (8)$$

$$\Delta = \epsilon - 3P_N, \quad C = \frac{\Delta}{\epsilon}, \quad (9)$$

where $\Upsilon_{\alpha,\beta} = \partial^2 P_N / \partial\alpha\partial\beta$ as defined in Refs. [105, 106].

Another quantity of interest in this study is the quark condensate for a given flavor:

$$\langle \bar{\psi}_f \psi_f \rangle_{T,\mu} = -N_c \int \frac{d^4k}{(2\pi)^4} \text{Tr}_D S_{T,\mu}^{(f)}(k), \quad (10)$$

where $S_{T,\mu}^{(f)}(k)$ is a T - and μ -dependent flavor- f quark propagator in momentum space, Tr_D means trace over Dirac indices and $N_c = 3$ is the number of colors. We recall that the quark condensate is the (quasi)order parameter of the QCD chiral phase transition; in the chiral limit, it is a true order parameter.

A. Finite quark chemical potential μ_q

For a nonzero quark chemical potential μ_q , the mean-field thermodynamic potential corresponding to the Lagrangian in Eq. (1) can be written as

$$\begin{aligned} \Omega(T, \mu_q) &= \frac{(M - m_0)}{4G} - 2N_c N_f \int_\Lambda \frac{d^3k}{(2\pi)^3} \omega(k) \\ &\quad - 4N_c N_f T \int_{\Lambda_T} \frac{d^3k}{(2\pi)^3} \left[\log \left(1 + e^{-(\omega(k) + \mu_q)/T} \right) \right. \\ &\quad \left. + \log \left(1 + e^{-(\omega(k) - \mu_q)/T} \right) \right], \end{aligned} \quad (11)$$

where $\omega(k) = (k^2 + M^2)^{1/2}$ and $N_f = 2$ are, respectively, the color and flavor numbers. To assess the consequences of cutting off momentum modes in finite integrals, we introduced in the above Λ_T to indicate either $\Lambda_T = \Lambda$ or $\Lambda_T \rightarrow \infty$. In the former case, one is cutting off momentum modes in finite integrals that do not require a regularization, as the explicit dependence of the integrals on T and μ_q makes them finite. In the latter case, all momentum modes contribute to the finite integrals. This procedure is similar to the one used in Ref. [85], although in that reference the authors restricted their analyses to the quark condensate as a function of μ_5 only and have not addressed causality violation issues, the main topic of the present study.

The gap equation for the constituent quark mass M is given by

$$\begin{aligned} M &= m_0 + 4N_c N_f G \int_\Lambda \frac{d^3k}{(2\pi)^3} \frac{M}{\omega(k)} \\ &\quad - 4N_c N_f G \int_{\Lambda_T} \frac{d^3k}{(2\pi)^3} \frac{M}{\omega(k)} [n_-(k) + n_+(k)], \end{aligned} \quad (12)$$

where $n_\mp(k)$ are the quark and antiquark Fermi-Dirac distributions:

$$n_\mp(k) = \frac{1}{e^{(\omega(k) \mp \mu_q)/T} + 1}. \quad (13)$$

While the first term in the gap equation (12) is ultraviolet divergent, the second is finite due to the Fermi-Dirac distributions that provide a natural cutoff for the high momentum modes. Even for $T = 0$ the second term is finite, since $n_-(T = 0, \mu_q) = \theta(k_F - k)$ and $n_+(T = 0, \mu_q) = 0$, where $k_F = (\mu_q^2 - M^2)^{1/2}$ is the Fermi momentum.

To compute the thermodynamical quantities of interest via Eqs. (7)–(9), with $\mu = \mu_q$ and $\rho = \rho_q$, we need the expressions for the entropy density s and quark number density ρ_q :

$$\begin{aligned} s &= 2N_c N_f \int_{\Lambda_T} \frac{d^3k}{(2\pi)^3} \left\{ \log [1 - n_-(k)] [1 - n_+(k)] \right. \\ &\quad \left. - \frac{\omega(k)}{T} [n_-(k) + n_+(k)] + \frac{\mu_q}{T} [n_-(k) - n_+(k)] \right\}, \end{aligned} \quad (14)$$

$$\rho_q = -2N_c N_f \int_{\Lambda_T} \frac{d^3k}{(2\pi)^3} [n_-(k) - n_+(k)]. \quad (15)$$

Here, we have only finite integrals as they involve the Fermi-Dirac distributions $n_\mp(k)$, which depend on T and μ .

B. Finite quark chiral chemical potential μ_5

The mean-field grand canonical potential at finite quark chiral potential μ_5 can be written as:

$$\begin{aligned} \Omega(T, \mu_5) &= \frac{(M - m_0)}{4G} - N_c N_f \sum_{s=\pm 1} \int_{\Lambda} \frac{d^3 k}{(2\pi)^3} \omega_s(k) \\ &\quad - 2N_c N_f T \sum_{s=\pm 1} \int_{\Lambda_T} \frac{d^3 k}{(2\pi)^3} \log \left(1 + e^{-\omega_s(k)/T} \right), \end{aligned} \quad (16)$$

where $\omega_s(k) = ((k + s\mu_5)^2 + M^2)^{1/2}$ are the eigenvalues of the Dirac Hamiltonian for quark helicities $s = \pm 1$. Again, one has a divergent integral and a finite integral, in which we introduced Λ and Λ_T . The gap equation for the constituent quark mass M , in this case, is given by:

$$\begin{aligned} M &= m_0 + 2N_c N_f G \sum_{s=\pm 1} \int_{\Lambda} \frac{d^3 k}{(2\pi)^3} \frac{M}{\omega_s(k)} \\ &\quad - 4N_c N_f G \int_{\Lambda_T} \frac{d^3 k}{(2\pi)^3} \frac{M}{\omega_s(k)} n_s(k), \end{aligned} \quad (17)$$

where $n_s(k)$ is the Fermi-Dirac distribution

$$n_s(k) = \frac{1}{e^{\omega_s(k)/T} + 1}. \quad (18)$$

The entropy density is given by

$$\begin{aligned} s &= 2N_c N_f \sum_{s=\pm 1} \int_{\Lambda_T} \frac{d^3 k}{(2\pi)^3} \left[\frac{\omega_s(k)}{T} n_s(k) \right. \\ &\quad \left. + \log \left(1 + e^{-\omega_s(k)/T} \right) \right]. \end{aligned} \quad (19)$$

The fact that we used s to indicate both the entropy density and quark chirality should not cause confusion as their meaning should be clear by the context in which they appear in the equations. Now, contrary to the baryon charge, the chiral charge is not a conserved quantity for massive quarks; thereby, the chiral density ρ_5 is not finite in the chirally broken phase of the NJL model and one needs a prescription to give physical meaning to ρ_5 . Here we follow the prescription of Ref. [101] and redefine ρ_5 as $\rho_{5N} = -\partial\Omega_N/\partial\mu_5$, where $\Omega_N(T, \mu_5) = \Omega(T, \mu_5) - \Omega_N(0, \mu_5)$, so that

$$\rho_{5N} = N_c N_f \sum_{s=\pm 1} \int_{\Lambda_T} \frac{d^3 k}{(2\pi)^3} \frac{s(k + s\mu_5)}{\omega_s(k)} (1 - 2n_s(k)). \quad (20)$$

For a thorough discussion on the meaning of such a renormalization in QCD, we direct the reader to Ref. [101]. The expressions for the speed of sound, specific heat, trace anomaly, and conformal measure are given by Eqs. (7)-(9) with μ replaced by μ_5 and ρ by ρ_{5N} .

III. NUMERICAL RESULTS

We adopted the following values for the free parameters of the model: $\Lambda = 587.9$ MeV, $m_0 = 5.6$ MeV and $G = 2.44/\Lambda^2$. These values were chosen to reproduce the phenomenological vacuum values of the pion decay constant $f_\pi = 92.4$ MeV, pion mass $m_\pi = 135$ MeV, and the chiral condensate $\langle \bar{u}u \rangle = (-240.8 \text{ MeV})^{1/3}$ [77]. In the following, we present the results for the speed of sound c_s , for zero chemical potentials $\mu_q = 0$ and $\mu_5 = 0$. Then, in the next two subsections, we consider nonzero values of μ_q and μ_5 and present results for c_V , Δ and C .

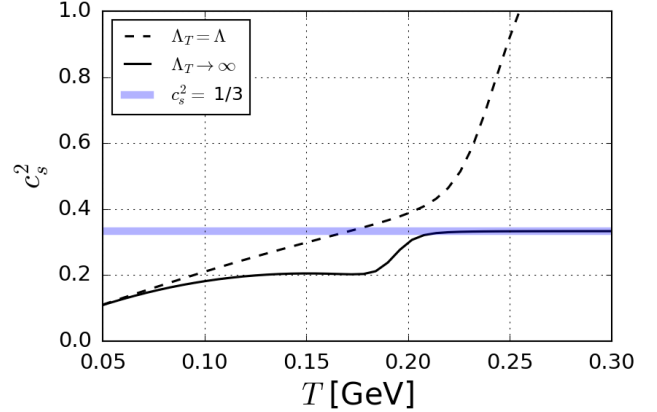


Figure 1. The speed of sound squared as a function of the temperature T for zero chemical potentials, $\mu_q = \mu_5 = 0$.

Figure 1 displays the temperature dependence of the squared speed of sound. The message the figure conveys is clear: Using $\Lambda_T = \Lambda$, with which one cuts off not only divergent integrals but also finite ones, the speed of sound exceeds the speed of light, thereby violating causality. Causality violation occurs for temperatures $T \gtrsim 255$ MeV, temperatures well in the range of those achieved in a heavy-ion collision. Moreover, the conformal limit $c_s^2 = 1/3$ is violated for temperatures $T > 170$ MeV. Now, when one keeps the whole contribution of the quark and antiquark Fermi-Dirac distributions, i.e. when using $\Lambda_T \rightarrow \infty$, the speed of sound approaches $c_s^2 = 1/3$, the conformal value, which is the correct value of the speed of sound of a high-temperature relativistic free gas of fermions—the Stefan-Boltzmann (SB) limit.

The relationship between the cutoff and the wrong behavior of the speed of sound can be qualitatively understood as follows. The system cannot build enough pressure to reach the SB limit when one eliminates quark high-momentum modes; for $T \gtrsim 150$ MeV, instead of increasing toward the SB limit, the pressure decreases with T . The energy density also decreases with T for $T \gtrsim 150$ MeV, but it decreases more rapidly than the pressure, which explains the rapid rise of c_s^2 for those temperatures. As we show in the following sections, where we consider the effects of finite μ_q and μ_5 , we obtain similar unphysical results not only for the speed of sound but also for other thermodynamical quantities, the reason for that is essentially the same as here for $\mu_q = \mu_5 = 0$.

A. Causality violation on the $T - \mu_q$ plane

We consider the T and μ_q dependence of c_s^2 using a three-dimensional momentum cutoff in both the divergent and finite integrals, i.e. we use $\Lambda_T = \Lambda$. Figure 2 displays the results for different values of the entropy to quark baryon density ratio, s/ρ_q . The red-shaded area represents the regions for which $c_s^2 > 1$. It is evident that c_s^2 is nonphysical for a wide range of phenomenologically relevant values of T and μ_q . Within this regularization scheme, the model can be safely used in the phenomenology of relativistic heavy-ions collisions ($\mu_q \sim 0$) only for temperatures up to $T \sim 250$ MeV, whereas in the phenomenology of quark or hybrid stars ($T \sim 0$) it can be safely used only for quark chemical potentials up to $\mu_q \sim 500$ MeV (that correspond to the baryon density $\rho_B \approx 7\rho_0$, where $\rho_0 = 0.16 fm^{-3}$ is the saturation density of nuclear matter).

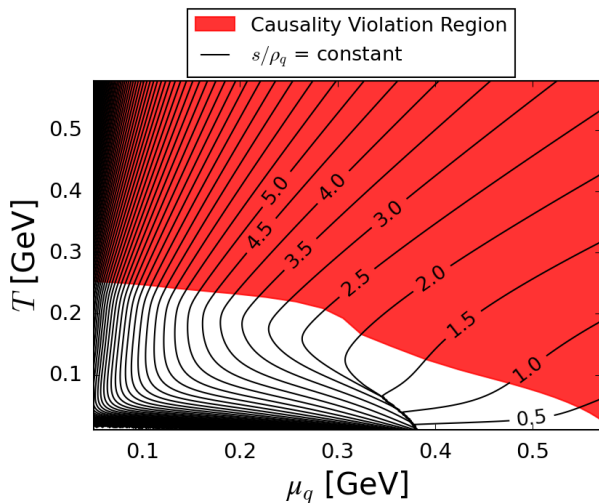


Figure 2. The red-shaded area identifies the region of causality violation ($c_s^2 > 1$) in the $T - \mu_q$ plane for constant values of entropy to quark baryon density ratios (black curves). These results are obtained using a three-dimensional cutoff in finite integrals, i.e. $\Lambda_T = \Lambda$.

Next, we consider the effect of the cutoff in the other observables of interest by comparing results obtained with $\Lambda_T = \Lambda$ and $\Lambda_T \rightarrow \infty$. First, we consider the specific heat c_V as a function of the temperature for $\mu_q = 0$ and $\mu_q = 200$ MeV. Figures 3 and 4 display, respectively, c_V/T^3 and c_V/Λ^3 ; we consider these two different normalizations to assess the high-temperature behavior of c_V better. Using $\Lambda_T = \Lambda$, one obtains nonphysical temperature dependence for c_V for temperatures $T \gtrsim 50$ MeV for both values of quark chemical potential considered. The fact that in this case c_V/T^3 is bigger at low temperatures for $\mu_q = 200$ MeV than for $\mu_q = 0$ is mainly due to the normalization by T^3 . In fact, c_V increases smoothly at low T as a function of μ_q , but it increases in a very artificial way when compared to the case with $\Lambda_T \rightarrow \infty$, as we can see in Fig. 4. The conclusion is that when using $\Lambda_T = \Lambda$ one obtains a wrong high-temperature behavior of the specific heat.

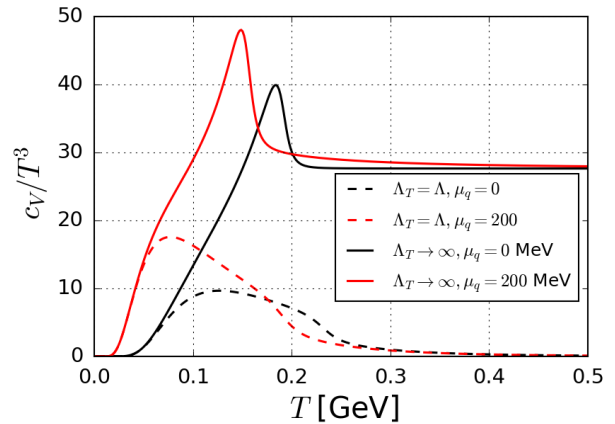


Figure 3. Specific heat normalized by T^3 as function of the temperature for two values of the quark baryon chemical potential μ_q .

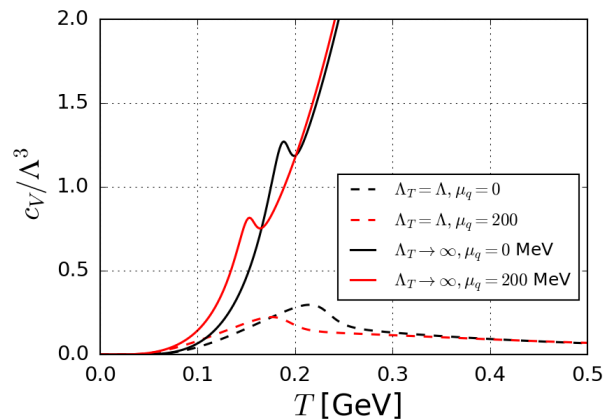


Figure 4. Specific heat normalized by Λ^3 as a function of the temperature for two values of the quark baryon chemical potential μ_q .

Finally, Figs. 5 and 6 display, respectively, the trace anomaly Δ normalized by T^4 and the conformal measure $C = \Delta/\epsilon$ as a function of temperature. Both quantities are expected to tend asymptotically to zero at large T . Recall that in the mean-field approximation, the effect of the interaction disappears at high temperatures due to the chiral restoration; see the first terms in Eqs. (11) and (16). Such a behavior happens when we use $\Lambda_T \rightarrow \infty$, but it does not happen when one uses $\Lambda_T = \Lambda$, for both finite and zero quark chemical potential. The pattern found in the case of $\Lambda_T \rightarrow \infty$, in both quantities, indicates that for asymptotically high temperatures, the theory behaves as a free theory, as expected within this mean-field approximation. The results obtained with $\Lambda_T = \Lambda$ and $\Lambda_T \rightarrow \infty$ start to deviate from each other at temperatures close to $T = 100$ MeV, in both Δ and C . Moreover, for temperatures close to $T = 200$ MeV, both quantities become negative when using $\Lambda_T = \Lambda$. Recent works [107–109] show that both the trace anomaly and conformal measure are positive quantities at finite density, indicating that using $\Lambda_T = \Lambda$ leads to wrong

high-temperature behavior for these quantities.

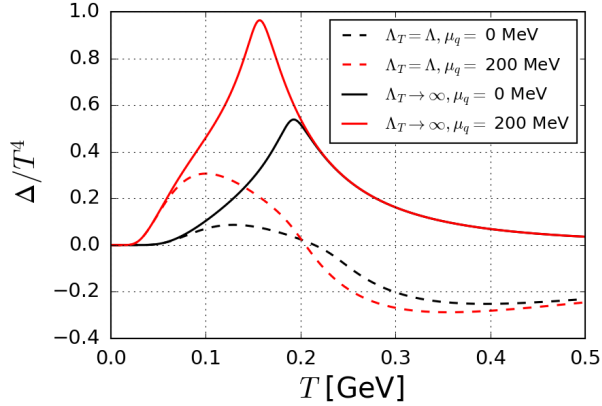


Figure 5. The normalized trace anomaly (or interaction measure) Δ as a function of the temperature for two values of the quark baryon chemical potential.

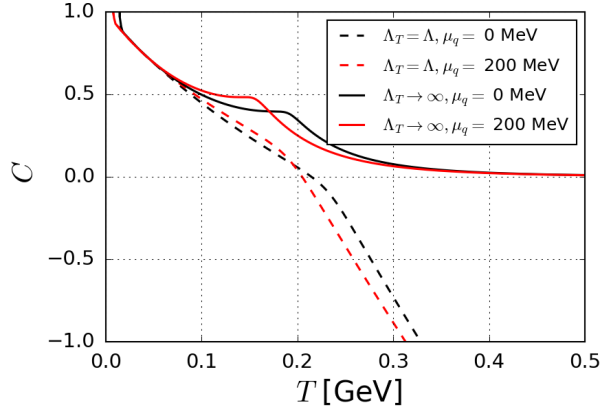


Figure 6. The conformal measure $C = \Delta/\epsilon$ as a function of the temperature for two values of the quark chemical potential.

We close this section by showing in Fig. 7 the quark condensate $\langle \bar{\psi}\psi \rangle$ computed with $\Lambda_T \rightarrow \infty$. The figure reveals that at both extremes of T and μ_q relevant to the phenomenologies of heavy collisions and neutron stars, one obtains a condensate that is still negative (the white region). This means that the constituent quark mass $M > m_0$ at those extremes; when $\langle \bar{\psi}\psi \rangle > 0$, one can have $M < m_0$.

B. Causality violation on the $T - \mu_5$ plane

In this section, we discuss causality violation for the case of finite chiral chemical potential, μ_5 . Again, we start analyzing the effect of using $\Lambda_T = \Lambda$ in the expression for the speed of sound; the results are displayed in Fig. 8 for $s/\rho_5 = 100$. Similar to Fig. 1, we have violation of causality ($c_s^2 > 1$) and of the conformal limit ($c_s^2 = 1/3$) at high temperatures. In contrast, these limits are fully obeyed when using $\Lambda_T \rightarrow \infty$.

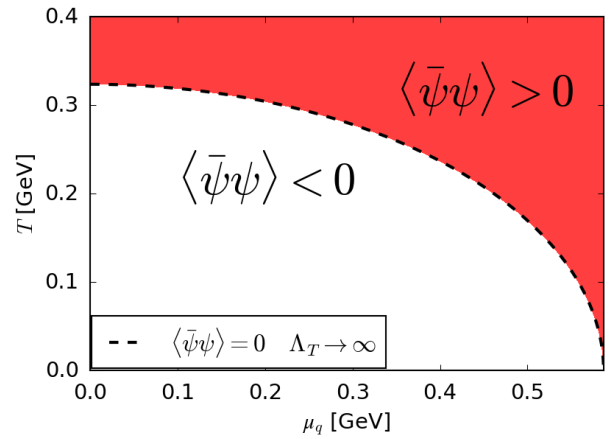


Figure 7. The quark condensate as a function of T and μ_q computed with $\Lambda_T \rightarrow \infty$.

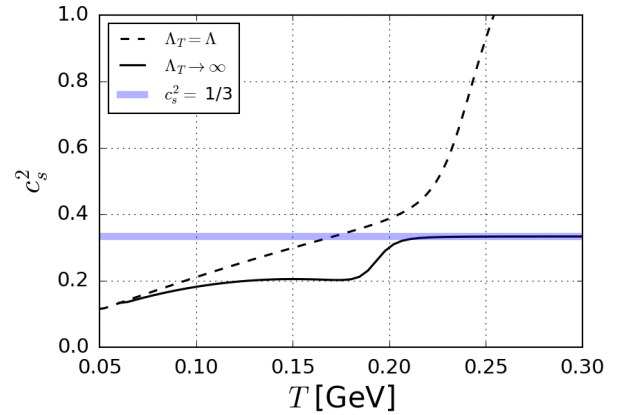


Figure 8. Speed of sound squared as a function of T for $s/\rho_5 = 100$.

The red-shaded area in Fig. 9 indicates the region in the $T - \mu_5$ plane, where $c_s^2 > 1$ for different values of the s/ρ_5 ratio. The situation is similar to that in Fig. 2, in that the temperature above which $c_s^2 > 1$ decreases with the corresponding chemical potential.

Next, we analyze the temperature dependence of the normalized specific heat C_V/T^3 and C_V/Λ^3 regarding the use of the different cutoff strategies. Figures 10 and 11 display the results for $\mu_5 = 0$ and $\mu_5 = 200$ MeV. Again, the wrong high-temperature behavior of these quantities is clear when using $\Lambda_T = \Lambda$. The results also indicate a milder dependence of C_V on μ_5 than on μ_q , using either $\Lambda_T = \Lambda$ or $\Lambda_T \rightarrow \infty$.

Finally, we plot the temperature dependence of Δ/T^4 and $C = \Delta/\epsilon$, respectively, in Figs. 12 and 13, for two values of chiral chemical potential, $\mu_5 = 0$ and $\mu_5 = 200$ MeV. These two quantities indicate very similar behavior when compared with Figs. 5 and 6. Clearly, the trace anomaly calculated with $\Lambda_T = \Lambda$ is negative for high temperatures. This does not happen when using $\Lambda_T \rightarrow \infty$. The conformal measure, with $\Lambda_T = \Lambda$, becomes negative at $T \sim 200$ MeV, which is very close to the value at $\mu_5 = 0$. In this temperature region,

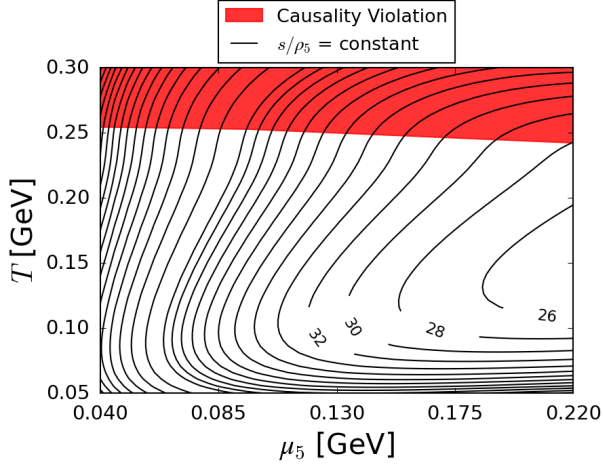


Figure 9. Regions of causality violation in the $T - \mu_5$ plane with curves of constant entropy, s/ρ_5 .

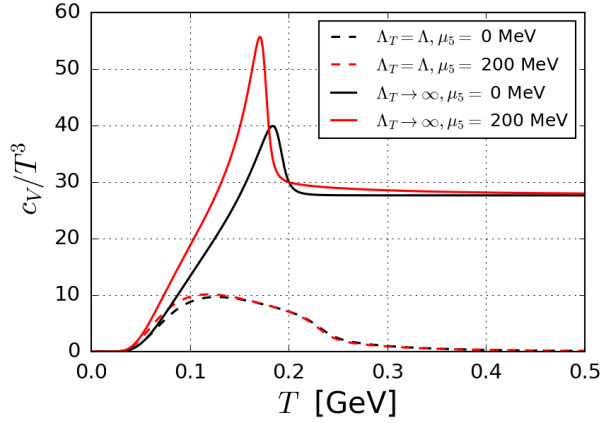


Figure 10. Specific heat divided by T^3 as a function of the temperature for two values of the chiral chemical potential μ_5 .

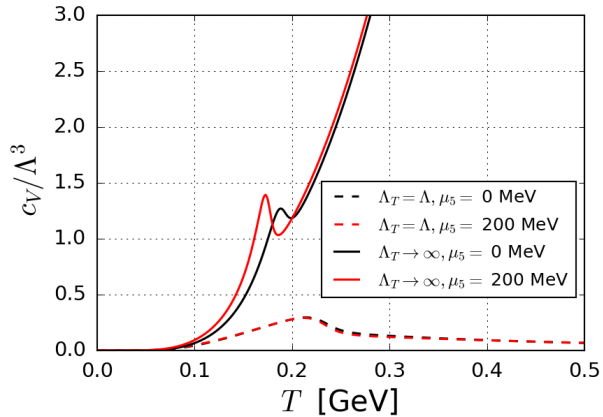


Figure 11. Specific heat divided by Λ^3 as a function of the temperature for two values of the chiral chemical potential μ_5 .

$c_s^2 > 1/3$. Since the $\mu_5 = 200$ MeV and $\mu_5 = 0$ situations

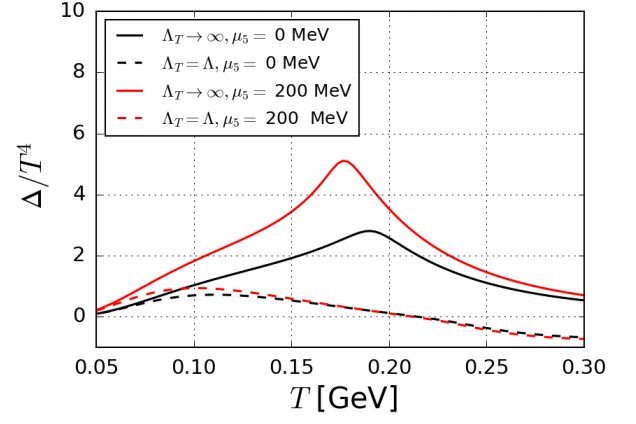


Figure 12. Results for normalized interaction measure (or trace anomaly) as a function of the temperature for two values of the chiral chemical potential.

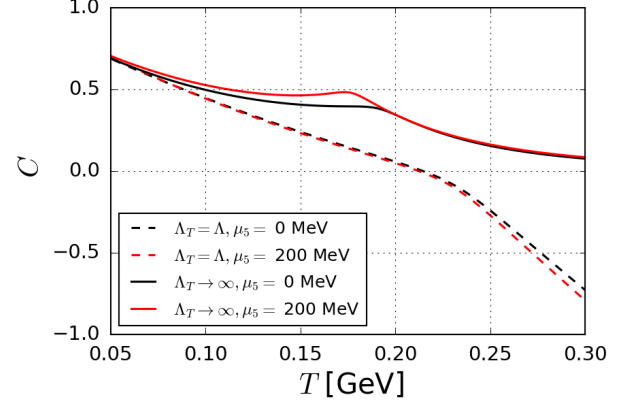


Figure 13. Conformal measure as a function of the temperature for two values of the chiral chemical potential.

are very similar, the conformal measure starts to disagree with the $\Lambda_T \rightarrow \infty$ case at $T \lesssim 100$ MeV, which indicates that the unphysical behavior induced by the regularization of the finite integrals happens for both $\mu_5 = 0$ and $\mu_5 \neq 0$.

To conclude this section, we mention that regularization issues also affect the temperature and density-dependent quark condensate or, equivalently, the constituent quark mass. For example, depending on the value of the cutoff, one can obtain negative constituent quark masses at high values of the temperature. Therefore, to obtain physical values for the masses and condensate, the cutoff must be tuned accordingly.

IV. CONCLUSIONS

In this work, we studied the implications of cutting moment integrals with a sharp three-momentum cutoff in the context of the two-flavor Nambu-Jona-Lasinio model. We compared the two procedures most commonly used in the literature: regularization only of the vacuum divergent integrals or regularization

of both divergent and finite integrals with the same cutoff. For a systematic discussion concerning the importance of the choice of the regularization procedure, we calculated the physical observables for both zero quark and chiral chemical potentials, $\mu_q = \mu_5 = 0$, and finite quark and chiral chemical potentials. We explored scenarios relevant to heavy-ion collisions and compact stars.

Our results indicated that causality violation and wrong high-temperature behavior of thermodynamical quantities are induced by the use of an ultraviolet cutoff in finite integrals depending on the Fermi-Dirac distributions. These problems happen in both $T - \mu$ and $T - \mu_5$ planes. On the other hand, when those finite integrals are not cut off, one obtains the expected conformal limit in the speed of sound in the high-temperature limit. The specific heat, trace anomaly, and conformal measure were also investigated in these scenarios. In the specific heat and trace anomaly, the behavior of free quark gas is not achieved if one regulates integrals containing the thermal distributions, with the conformal measure presenting negative values for $T \gtrsim 250$ MeV.

The analyses in this work indicate that, depending on the choice of the regularization, NJL-type models might induce artificial and unphysical behavior of physical observables. NJL-

type models have been instrumental in guiding our intuition regarding chiral symmetry in vacuum and in matter; ignoring these regularization issues can lead to confusion and misguidance.

ACKNOWLEDGMENTS

This work was partially supported by Conselho Nacional de Desenvolvimento Científico e Tecnológico (CNPq), Grants Nos. 131212/2020-6 (A.E.B.P.), 309598/2020-6 (R.L.S.F.), 304518/2019-0 (S.S.A.), 309262/2019-4; Coordenação de Aperfeiçoamento de Pessoal de Nível Superior (CAPES) Finance Code 001 and Fundação Carlos Chagas Filho de Amparo à Pesquisa do Estado do Rio de Janeiro (FAPERJ), Grant No. SEI-260003/019544/2022 (W.R.T); Fundação de Amparo à Pesquisa do Estado do Rio Grande do Sul (FAPERGS), Grants Nos. 19/2551-0000690-0 and 19/2551-0001948-3 (R.L.S.F.); Fundação de Amparo à Pesquisa do Estado de São Paulo (FAPESP), grant no. 2018/25225-9 (G.K.). The work is also part of the project Instituto Nacional de Ciência e Tecnologia - Física Nuclear e Aplicações (INCT - FNA), Grant No. 464898/2014-5.

-
- [1] R. Snellings, *New J. Phys.* **13**, 055008 (2011). doi:10.1088/1367-2630/13/5/055008
- [2] W. Busza, K. Rajagopal, W. van der Schee, *Ann. Rev. Nucl. Part. Sci.* **68**, 339 (2018). doi:10.1146/annurev-nucl-101917-020852
- [3] H. Elfner, B. Müller, The exploration of hot and dense nuclear matter: Introduction to relativistic heavy-ion physics, 2210.12056 (2022)
- [4] P. Braun-Munzinger, V. Koch, T. Schäfer, J. Stachel, *Phys. Rep.* **621**, 76 (2016). doi:10.1016/j.physrep.2015.12.003
- [5] A. Sorensen, D. Oliinychenko, V. Koch, L. McLerran, *Phys. Rev. Lett.* **127**, 042303 (2021). doi:10.1103/PhysRevLett.127.042303
- [6] J.J. Li, A. Sedrakian, M. Alford, *Phys. Rev. D* **101**(6), 063022 (2020). doi:10.1103/PhysRevD.101.063022
- [7] M.G. Alford, S. Han, K. Schwenzer, *J. Phys. G* **46**(11), 114001 (2019). doi:10.1088/1361-6471/ab337a
- [8] E. Lope Oter, A. Windisch, F.J. Llanes-Estrada, M. Alford, *J. Phys. G* **46**(8), 084001 (2019). doi:10.1088/1361-6471/ab2567
- [9] J.J. Li, A. Sedrakian, M. Alford, *Phys. Rev. D* **104**(12), L121302 (2021). doi:10.1103/PhysRevD.104.L121302. [Erratum: *Phys.Rev.D* 105, 109901 (2022)]
- [10] S.K. Greif, G. Raaijmakers, K. Hebeler, A. Schwenk, A.L. Watts, *Mon. Not. Roy. Astron. Soc.* **485**(4), 5363 (2019). doi:10.1093/mnras/stz654
- [11] D.C. Duarte, S. Hernandez-Ortiz, K.S. Jeong, *Phys. Rev. C* **102**(6), 065202 (2020). doi:10.1103/PhysRevC.102.065202
- [12] T. Kojo, *AAPPS Bull.* **31**(1), 11 (2021). doi:10.1007/s43673-021-00011-6
- [13] J.R. Stone, V. Dexheimer, P.A.M. Guichon, A.W. Thomas, S. Typel, *Mon. Not. Roy. Astron. Soc.* **502**(3), 3476 (2021). doi:10.1093/mnras/staa4006
- [14] I. Tews, J. Margueron, S. Reddy, *Phys. Rev. C* **98**(4), 045804 (2018). doi:10.1103/PhysRevC.98.045804
- [15] T. Kojo, P.D. Powell, Y. Song, G. Baym, *Phys. Rev. D* **91**(4), 045003 (2015). doi:10.1103/PhysRevD.91.045003
- [16] M.G. Alford, S. Han, M. Prakash, *Phys. Rev. D* **88**(8), 083013 (2013). doi:10.1103/PhysRevD.88.083013
- [17] P. Bedaque, A.W. Steiner, *Phys. Rev. Lett.* **114**(3), 031103 (2015). doi:10.1103/PhysRevLett.114.031103
- [18] E.D. Van Oeveren, J.L. Friedman, *Phys. Rev. D* **95**(8), 083014 (2017). doi:10.1103/PhysRevD.95.083014
- [19] C. Margaritis, P.S. Koliogiannis, C.C. Moustakidis, *Phys. Rev. D* **101**(4), 043023 (2020). doi:10.1103/PhysRevD.101.043023
- [20] K. Otto, M. Oertel, B.J. Schaefer, *Phys. Rev. D* **101**(10), 103021 (2020). doi:10.1103/PhysRevD.101.103021
- [21] P. Landry, R. Essick, K. Chatziioannou, *Phys. Rev. D* **101**(12), 123007 (2020). doi:10.1103/PhysRevD.101.123007
- [22] N. Jokela, M. Järvinen, G. Nijs, J. Remes, *Phys. Rev. D* **103**(8), 086004 (2021). doi:10.1103/PhysRevD.103.086004
- [23] C.C. Moustakidis, T. Gaitanos, C. Margaritis, G.A. Lalazissis, *Phys. Rev. C* **95**(4), 045801 (2017). doi:10.1103/PhysRevC.95.045801. [Erratum: *Phys.Rev.C* 95, 059904 (2017)]
- [24] J.C. Jiménez, E.S. Fraga, *Phys. Rev. D* **104**(1), 014002 (2021). doi:10.1103/PhysRevD.104.014002
- [25] E. Annala, T. Gorda, A. Kurkela, J. Nättilä, A. Vuorinen, *Nature Phys.* **16**(9), 907 (2020). doi:10.1038/s41567-020-0914-9
- [26] M. Hippert, E.S. Fraga, J. Noronha, *Phys. Rev. D* **104**(3), 034011 (2021). doi:10.1103/PhysRevD.104.034011
- [27] M. Ferreira, R. Câmara Pereira, C. Providência, *Phys. Rev. D* **102**(8), 083030 (2020). doi:10.1103/PhysRevD.102.083030
- [28] H. Tan, T. Dore, V. Dexheimer, J. Noronha-Hostler, N. Yunes, *Phys. Rev. D* **105**(2), 023018 (2022). doi:10.1103/PhysRevD.105.023018
- [29] I. Tews, J. Margueron, S. Reddy, *Eur. Phys. J. A* **55**(6), 97 (2019). doi:10.1140/epja/i2019-12774-6

- [30] P. Jaikumar, A. Semposki, M. Prakash, C. Constantinou, Phys. Rev. D **103**(12), 123009 (2021). doi:10.1103/PhysRevD.103.123009
- [31] C. Constantinou, S. Han, P. Jaikumar, M. Prakash, Phys. Rev. D **104**(12), 123032 (2021). doi:10.1103/PhysRevD.104.123032
- [32] S. Han, M.A.A. Mamun, S. Lalit, C. Constantinou, M. Prakash, Phys. Rev. D **100**(10), 103022 (2019). doi:10.1103/PhysRevD.100.103022
- [33] Y.L. Ma, M. Rho, Phys. Rev. D **100**(11), 114003 (2019). doi:10.1103/PhysRevD.100.114003
- [34] L. McLerran, S. Reddy, Phys. Rev. Lett. **122**(12), 122701 (2019). doi:10.1103/PhysRevLett.122.122701
- [35] I. Tews, T. Krüger, K. Hebeler, A. Schwenk, Phys. Rev. Lett. **110**(3), 032504 (2013). doi:10.1103/PhysRevLett.110.032504
- [36] K. Hebeler, J.M. Lattimer, C.J. Pethick, A. Schwenk, Astrophys. J. **773**, 11 (2013). doi:10.1088/0004-637X/773/1/11
- [37] B.A. Freedman, L.D. McLerran, Phys. Rev. D **16**, 1147 (1977). doi:10.1103/PhysRevD.16.1147
- [38] A. Kurkela, P. Romatschke, A. Vuorinen, Phys. Rev. D **81**, 105021 (2010). doi:10.1103/PhysRevD.81.105021
- [39] E.S. Fraga, A. Kurkela, A. Vuorinen, Astrophys. J. Lett. **781**(2), L25 (2014). doi:10.1088/2041-8205/781/2/L25
- [40] I. Tews, J. Carlson, S. Gandolfi, S. Reddy, Astrophys. J. **860**(2), 149 (2018). doi:10.3847/1538-4357/aac267
- [41] G. Baym, T. Hatsuda, T. Kojo, P.D. Powell, Y. Song, T. Takatsuka, Rept. Prog. Phys. **81**(5), 056902 (2018). doi:10.1088/1361-6633/aaae14
- [42] B. Reed, C.J. Horowitz, Phys. Rev. C **101**(4), 045803 (2020). doi:10.1103/PhysRevC.101.045803
- [43] A. Kanakis-Pegios, P.S. Koliogiannis, C.C. Moustakidis, Phys. Rev. C **102**(5), 055801 (2020). doi:10.1103/PhysRevC.102.055801
- [44] C. Drischler, S. Han, J.M. Lattimer, M. Prakash, S. Reddy, T. Zhao, Phys. Rev. C **103**(4), 045808 (2021). doi:10.1103/PhysRevC.103.045808
- [45] P. Huovinen, P. Petreczky, C. Schmidt, Nucl. Phys. A **931**, 769 (2014). doi:10.1016/j.nuclphysa.2014.08.069
- [46] M. Motta, R. Stiele, W.M. Alberico, A. Beraudo, Eur. Phys. J. C **80**(8), 770 (2020). doi:10.1140/epjc/s10052-020-8218-x
- [47] B.I. Abelev, et al., Phys. Rev. C **79**, 034909 (2009). doi:10.1103/PhysRevC.79.034909
- [48] L. Adamczyk, et al., Phys. Rev. C **96**(4), 044904 (2017). doi:10.1103/PhysRevC.96.044904
- [49] D. Blaschke, EPJ Web Conf. **138**, 01004 (2017). doi:10.1051/epjconf/201713801004
- [50] S. Ejiri, F. Karsch, E. Laermann, C. Schmidt, Phys. Rev. D **73**, 054506 (2006). doi:10.1103/PhysRevD.73.054506
- [51] M. Bluhm, B. Kampfer, R. Schulze, D. Seipt, U. Heinz, Phys. Rev. C **76**, 034901 (2007). doi:10.1103/PhysRevC.76.034901
- [52] A. Steiner, M. Prakash, J.M. Lattimer, Phys. Lett. B **486**, 239 (2000). doi:10.1016/S0370-2693(00)00780-2
- [53] M. Marianti, M. Orsaria, H. Vucetich, Astron. Astrophys. **601**, A21 (2017). doi:10.1051/0004-6361/201629315
- [54] M. Marianti, M. Orsaria, H. Vucetich, Int. J. Mod. Phys. Conf. Ser. **45**, 1760041 (2017). doi:10.1142/S2010194517600412
- [55] C. Constantinou, B. Muccioli, M. Prakash, J.M. Lattimer, Phys. Rev. C **89**(6), 065802 (2014). doi:10.1103/PhysRevC.89.065802
- [56] C. Constantinou, B. Muccioli, M. Prakash, J.M. Lattimer, Phys. Rev. C **92**(2), 025801 (2015). doi:10.1103/PhysRevC.92.025801
- [57] D.J. Gross, R.D. Pisarski, L.G. Yaffe, Rev. Mod. Phys. **53**, 43 (1981). doi:10.1103/RevModPhys.53.43
- [58] H. Aoyama, H. Goldberg, Z. Ryzak, Phys. Rev. Lett. **60**, 1902 (1988). doi:10.1103/PhysRevLett.60.1902
- [59] K. Fukushima, D.E. Kharzeev, H.J. Warringa, Phys. Rev. D **78**, 074033 (2008). doi:10.1103/PhysRevD.78.074033
- [60] D.E. Kharzeev, H.J. Warringa, Phys. Rev. D **80**, 034028 (2009). doi:10.1103/PhysRevD.80.034028
- [61] D. Kharzeev, Phys. Lett. B **633**, 260 (2006). doi:10.1016/j.physletb.2005.11.075
- [62] D.E. Kharzeev, J. Liao, S.A. Voloshin, G. Wang, Prog. Part. Nucl. Phys. **88**, 1 (2016). doi:10.1016/j.ppnp.2016.01.001
- [63] X.G. Huang, Rept. Prog. Phys. **79**(7), 076302 (2016). doi:10.1088/0034-4885/79/7/076302
- [64] J. Zhao, F. Wang, Prog. Part. Nucl. Phys. **107**, 200 (2019). doi:10.1016/j.ppnp.2019.05.001
- [65] M. Abdallah, et al., Phys. Rev. C **105**(1), 014901 (2022). doi:10.1103/PhysRevC.105.014901
- [66] N. Yamanaka, arXiv preprint arXiv:2212.11820 (2022)
- [67] N. Yamanaka, arXiv preprint arXiv:2212.10994 (2022)
- [68] M. Ruggieri, Z.Y. Lu, G.X. Peng, Phys. Rev. D **94**(11), 116003 (2016). doi:10.1103/PhysRevD.94.116003
- [69] M. Ruggieri, G.X. Peng, Phys. Rev. D **93**(9), 094021 (2016). doi:10.1103/PhysRevD.93.094021
- [70] L.K. Yang, X.F. Luo, J. Segovia, H.S. Zong, Symmetry **12**(12) (2020). doi:10.3390/sym12122095
- [71] A. Yamamoto, Phys. Rev. Lett. **107**, 031601 (2011). doi:10.1103/PhysRevLett.107.031601
- [72] R.L.S. Farias, D.C. Duarte, G.a. Krein, R.O. Ramos, Phys. Rev. D **94**(7), 074011 (2016). doi:10.1103/PhysRevD.94.074011
- [73] Y. Nambu, G. Jona-Lasinio, Phys. Rev. **122**, 345 (1961). doi:10.1103/PhysRev.122.345
- [74] Y. Nambu, G. Jona-Lasinio, Phys. Rev. **124**, 246 (1961). doi:10.1103/PhysRev.124.246
- [75] S.P. Klevansky, Rev. Mod. Phys. **64**, 649 (1992). doi:10.1103/RevModPhys.64.649
- [76] T. Hatsuda, T. Kunihiro, Phys. Rept. **247**, 221 (1994). doi:10.1016/0370-1573(94)90022-1
- [77] M. Buballa, Physics Reports **407**(4-6), 205–376 (2005). doi:10.1016/j.physrep.2004.11.004
- [78] A. Bandyopadhyay, R.L.S. Farias, Eur. Phys. J. ST **230**(3), 719 (2021). doi:10.1140/epjs/s11734-021-00023-1
- [79] Q.W. Wang, C. shi, H.S. Zong, Chin. Phys. C **45**(8), 084110 (2021). doi:10.1088/1674-1137/ac0329
- [80] Z.Q. Wu, J.L. Ping, H.S. Zong, Chin. Phys. C **45**(6), 064102 (2021). doi:10.1088/1674-1137/abefc3
- [81] T. Zhao, W. Zheng, F. Wang, C.M. Li, Y. Yan, Y.F. Huang, H.S. Zong, Phys. Rev. D **100**(4), 043018 (2019). doi:10.1103/PhysRevD.100.043018
- [82] B. Sheng, Y. Wang, X. Wang, L. Yu, Phys. Rev. D **103**(9), 094001 (2021). doi:10.1103/PhysRevD.103.094001
- [83] B.k. Sheng, X. Wang, L. Yu, Phys. Rev. D **105**(3), 034003 (2022). doi:10.1103/PhysRevD.105.034003
- [84] S. Mao, Y. Wu, P. Zhuang, Strongly Interacting Matter in Magnetic Field. doi:10.7566/JPSCP.20.011009. URL <https://journals.jps.jp/doi/abs/10.7566/JPSCP.20.011009>
- [85] L. Yu, H. Liu, M. Huang, Phys. Rev. D **94**(1), 014026 (2016). doi:10.1103/PhysRevD.94.014026
- [86] Z.Q. Wu, Chao-Shi, J.L. Ping, H.S. Zong, Phys. Rev. D **101**(7), 074008 (2020). doi:10.1103/PhysRevD.101.074008
- [87] L.K. Yang, X. Luo, H.S. Zong, Phys. Rev. D **100**(9), 094012 (2019). doi:10.1103/PhysRevD.100.094012
- [88] Z.F. Cui, J.L. Zhang, H.S. Zong, Sci. Rep. **7**, 45937 (2017). doi:10.1038/srep45937

- [89] P. Costa, H. Hansen, M. Ruivo, C. de Sousa, *Phys. Rev. D* **81**, 016007 (2010). doi:10.1103/PhysRevD.81.016007
- [90] P. Costa, M.C. Ruivo, C.A. de Sousa, H. Hansen, *Symmetry* **2**, 1338 (2010). doi:10.3390/sym2031338
- [91] R. Marty, E. Bratkovskaya, W. Cassing, J. Aichelin, H. Berrehrah, *J. Phys. Conf. Ser.* **509**, 012052 (2014). doi:10.1088/1742-6596/509/1/012052
- [92] P. Zhuang, J. Hufner, S. Klevansky, *Nucl. Phys. A* **576**, 525 (1994). doi:10.1016/0375-9474(94)90743-9
- [93] J. Chao, P. Chu, M. Huang, *Phys. Rev. D* **88**, 054009 (2013). doi:10.1103/PhysRevD.88.054009
- [94] L. Yu, H. Liu, M. Huang, *Phys. Rev. D* **90**(7), 074009 (2014). doi:10.1103/PhysRevD.90.074009
- [95] V.V. Braguta, E.M. Ilgenfritz, A.Y. Kotov, B. Petersson, S.A. Skinderev, *Phys. Rev. D* **93**(3), 034509 (2016). doi:10.1103/PhysRevD.93.034509
- [96] V.V. Braguta, V.A. Goy, E.M. Ilgenfritz, A.Y. Kotov, A.V. Molochkov, M. Muller-Preussker, B. Petersson, *JHEP* **06**, 094 (2015). doi:10.1007/JHEP06(2015)094
- [97] M. Ruggieri, *Phys. Rev. D* **84**, 014011 (2011). doi:10.1103/PhysRevD.84.014011
- [98] K. Fukushima, M. Ruggieri, R. Gatto, *Phys. Rev. D* **81**, 114031 (2010). doi:10.1103/PhysRevD.81.114031
- [99] Z.F. Cui, I.C. Cloet, Y. Lu, C.D. Roberts, S.M. Schmidt, S.S. Xu, H.S. Zong, *Phys. Rev. D* **94**, 071503 (2016). doi:10.1103/PhysRevD.94.071503
- [100] M.N. Chernodub, A.S. Nedelin, *Phys. Rev. D* **83**, 105008 (2011). doi:10.1103/PhysRevD.83.105008
- [101] M. Ruggieri, M.N. Chernodub, Z.Y. Lu, *Phys. Rev. D* **102**(1), 014031 (2020). doi:10.1103/PhysRevD.102.014031
- [102] V.V. Braguta, A.Y. Kotov, *Phys. Rev. D* **93**(10), 105025 (2016). doi:10.1103/PhysRevD.93.105025
- [103] Y. Lu, Z.F. Cui, Z. Pan, C.H. Chang, H.S. Zong, *Phys. Rev. D* **93**(7), 074037 (2016). doi:10.1103/PhysRevD.93.074037
- [104] C. Shi, X.T. He, W.B. Jia, Q.W. Wang, S.S. Xu, H.S. Zong, *JHEP* **06**, 122 (2020). doi:10.1007/JHEP06(2020)122
- [105] R. Marty, E. Bratkovskaya, W. Cassing, J. Aichelin, H. Berrehrah, *Phys. Rev. C* **88**, 045204 (2013). doi:10.1103/PhysRevC.88.045204
- [106] S. Floerchinger, M. Martinez, *Phys. Rev. C* **92**(6), 064906 (2015). doi:10.1103/PhysRevC.92.064906
- [107] Y. Fujimoto, K. Fukushima, L.D. McLerran, M. Praszalowicz, arXiv preprint arXiv: 2207.06753
- [108] M.B. Pinto, arXiv preprint arXiv: 2211.11071
- [109] M.B. Pinto, arXiv preprint arXiv: 2208.06911